Polymer 49 (2008) 5670–5675

Contents lists available at ScienceDirect

Polymer

journal homepage: www.elsevier.com/locate/polymer

Unique crystallization behavior of poly(L-lactide)/poly(D-lactide) stereocomplex depending on initial melt states

Yong He [a,b], Ying Xu [a], Jia Wei [a], Zhongyong Fan [a], Suming Li [a,b,*]

[a] Department of Materials Science, Fudan University, Shanghai 200433, China
[b] University Montpellier I, Max Mousseron Institute on Biomolecules, UMR CNRS 5247, Faculty of Pharmacy, 34060 Montpellier, France

ARTICLE INFO

Article history:
Received 30 September 2008
Received in revised form
16 October 2008
Accepted 17 October 2008
Available online 29 October 2008

Keywords:
Stereocomplex
Polylactide
Crystallization

ABSTRACT

A unique crystallization behavior of poly(L-lactide) (PLLA)/poly(D-lactide) (PDLA) stereocomplex was observed when a PLLA/PDLA blend (50/50) was subjected to specific melting conditions. PLLA and PDLA were synthesized by ring opening polymerization of L- or D-lactide using zinc lactate as catalyst. PLLA/PDLA blend was prepared through solution mixing followed by vacuum drying. The blend was melted under various melting conditions and subsequent crystallization behaviors were analyzed by using DSC, XRD, NMR and ESEM. Stereocomplex was exclusively formed from the 50/50 blend of PLLA and PDLA with relatively low molecular weights. Surprisingly, stereocomplex crystallization was distinctly depressed when higher melting temperature and longer melting period were applied, in contrast to homopolymer crystallization. Considering predominant interactions between PLLA and PDLA chains, a novel model of melting process is proposed to illustrate this behavior. It is assumed that PLLA and PDLA chain couples would preserve their interactions (melt memory) when the stereocomplex crystal melts smoothly, thus resulting in a heterogeneous melt which can easily crystallize. The melt could gradually become homogeneous at higher temperature or longer melting time. The strong interactions between PLLA and PDLA chain segments are randomly distributed in a homogeneous melt, thus preventing subsequent stereocomplex crystallization. However, the homogeneous melt can recover its ability to crystallize via dissolution in a solvent.

1. Introduction

Polylactide (PLA) has received wide attention in the medical and pharmaceutical fields due to its biodegradability, biocompatibility, and good mechanical properties [1,2]. PLA can be used to fabricate various osteosynthetic devices, drug delivery systems and tissue engineering scaffolds, etc. The degradation characteristics of PLA, which are of major importance for various applications, mainly depend on the crystalline morphology and crystallinity. Lactide exists in three isomeric forms, i.e. L-lactide, D-lactide and meso-lactide, which allows to prepare various PLA homo- and stereo-copolymers with dramatically different properties by adjusting L/D ratios in the monomer feeds.

Since Ikada et al. reported stereocomplex formation between enantiomeric poly(L-lactide) (PLLA) and poly(D-lactide) (PDLA) [3], many researchers have focused on its significance for PLA-based materials, in particular on the physical properties, thermal properties and hydrolysis resistance [4–6]. In the meantime, there are a great number of patents dealing with stereocomplex processing technologies because of the potential applications [7,8]. Stereocomplex crystallites exhibit much higher crystal growth rate and shorter induction period than either PLLA or PDLA [9,10]. The melting point of the stereocomplex is *ca.* 50 °C higher than that of pure PLLA or PDLA [3,11]. Single crystals of the stereocomplex favor a triangular shape with a β-form 3_1-helice packing of opposite configurations alternating side by side [12,13]. However, while stereocomplex can be obtained from the melt, the melting conditions and the melt state prior to crystallization have not been investigated, so far. In fact, it was assumed that melt state should not account for the stereocomplex crystallization [9–13].

Recently, several reports have focused on the relationship between polymer crystallization and heterogeneous melt [14–16]. Lippits et al. reported that disentangled chain segments of polyethylene (PE) crystallize from heterogeneous melt much faster than entangled chains from homogeneous melt [15]. Entanglements formed during homogenization of heterogeneous melt could retard the crystallization. Comparatively, we can assume that the spatial distribution of interaction regions during homogenization of PLLA/PDLA heterogeneous melt would affect the crystallization process.

* Corresponding author. University Montpellier I, Max Mousseron Institute on Biomolecules, UMR CNRS 5247, Faculty of Pharmacy, 34060 Montpellier, France.
E-mail address: lisuming@univ-montp1.fr (S. Li).

0032-3861/$ – see front matter © 2008 Elsevier Ltd. All rights reserved.
doi:10.1016/j.polymer.2008.10.028

Indeed, it was found that stereocomplex crystallization was distinctly depressed when higher melting temperature and longer melting period were applied. Since interactions between PLA chain segments of opposite configurations are stronger than those of the same configurations, homogenization of spatial distribution of interaction regions in PLLA/PDLA melt would prevent PLLA and PDLA chain segments from coupling and being involved into crystallization frontier, and thus depress stereocomplex crystallization.

The mechanisms, by which polymer melt of high conformational entropy transform into a semicrystalline state of low entropy, have been previously studied [17]. Several researchers have reported that polymer crystallization from the melt may start from initial transient state (or named as precursors, mesomorphic seeds) [18–20]. And "melt memory" has been proposed to describe the behavior, i.e. a polymer in melt state might retain a partial memory of its former crystalline structure [21–23]. Therefore, melt state appears as an important factor in polymer crystallization.

In our previous studies, we have reported the basic crystallization behaviors of PLLA with different molecular weights [24,25]. In this work, relatively low molecular weight (M_n) PLLA and PDLA (in the order of 10^4 g/mol) were synthesized since stereocomplex is exclusively formed when the M_n of both PLLA and PDLA is in the order of 10^3–10^4 [11]. The relationship between the melt state and stereocomplex crystallization is reported herein.

2. Experimental section

2.1. Materials

L-lactide and D-lactide were purchased from Purac (The Netherlands). Zinc lactate and sodium azide were obtained from Merck. Trizma base, Trizma/HCl and proteinase K in the form of lyophilized powder (30 U/mg) were supplied by Sigma.

2.2. Methods

The synthesis of PLLA and PDLA was previously described [24,25]. PLLA and PDLA were synthesized by ring opening polymerization at 140 °C of L-lactide or D-lactide, using zinc lactate as catalyst and ethylene glycol as co-initiator to control the M_n. The molecular characteristics of PLLA and PDLA utilized in this study are listed in Table 1.

The PLLA/PDLA blend used for crystallization experiments was prepared as follows. Briefly, PLLA and PDLA solutions were separately prepared with a concentration of 1.0 g/dL, using methylene chloride as solvent. 10 mL of both solutions were then mixed under vigorous stirring. Then solvent was allowed to evaporate under room temperature for 3 days and the obtained sample was further vacuum dried up to constant weight.

2.3. Measurements

Size-exclusion chromatography (SEC) measurements were performed with a Waters apparatus equipped with a refractive index detector. Chloroform was used as the mobile phase at a flow rate of 1.0 mL/min. 20 μL of 1% (w/v) solution were injected for each analysis. The columns were calibrated with polystyrene standards (Polysciences).

Table 1
Characteristics of PLLA and PDLA homopolymers.

Sample	M_w (g/mol)	M_w/M_n	$[\alpha]_{20}^D$ (°)	T_g (°C)	T_{cc} (°C)	ΔH_c (J/g)	T_m (°C)	ΔH_m (J/g)
PLLA	3.6×10^4	1.4	−153	57.1	102.8	42.4	165.8	54.4
PDLA	1.9×10^4	1.4	154	55.4	100.1	35.0	160.3	41.1

Specific rotation of PLA ($[\alpha]_{20}^D$) was measured in chloroform at a concentration of 8.6 g/L and 20 °C by using a WZG-2S polarimeter.

X-ray diffraction spectra were registered with a Philips diffractometer composed of Cu Kα ($\lambda = 1.54$ Å) source, a quartz monochromator, and a goniometric plate.

^{13}C NMR spectra were recorded on a VAVCE-DMX 500 Spectrometer, operating at 125 MHz. $CDCl_3$ was used as solvent.

DSC analysis was performed with a Perkin–Elmer instrument DSC 6 calibrated with indium. The heating/cooling rate was fixed at 10 °C/min. The glass transition, cold crystallization and melting temperatures (T_g, T_{cc} and T_m, respectively) and enthalpies of crystallization and melting (ΔH_c and ΔH_m, respectively) were determined from amorphous PLLA and PDLA. The thermal properties of both polymers are summarized in Table 1.

The morphology of enzymatically etched samples was examined by using a Philips XL30 ESEM under reduced pressure below 1 torr. Each sample was placed in a vial filled with 10 mL of pH 8.6 Tris buffer (0.05 M) containing 2.0 mg of proteinase K and 2.0 mg of sodium azide. The vials were placed in an oven thermostated at 37 °C. After 3 days, the samples were withdrawn, gently washed with distilled water, and examined by using ESEM.

3. Results and discussion

Fig. 1 presents the thermal behaviors of the PLLA/PDLA blend. In the first run, only a T_m was detected at 215.9 °C with ΔH_m of 64.2 J/g. The melted sample was kept at 230 °C for 1 min, taken out and immediately immersed in liquid nitrogen to be made amorphous. In the second heating process, T_g and T_{cc} appeared at 53.1 and 95.9 °C, respectively. T_m decreased to 186.8 °C and ΔH_m to 26.0 J/g. The same procedure was applied for the third run which exhibits a T_g at 50.9 °C, a very weak cold crystallization around 130 °C and a very weak melting at 173.0 °C with ΔH_m of *ca.* 1.0 J/g.

Tsuji and Ikada previously reported that the melting of stereocomplex crystallites occurs at 220–230 °C with ΔH_m of 68–86 J/g [3,9–11]. The authors estimated the equilibrium melting temperature (T_m^0) of PLA stereocomplex crystallites to be 279 °C by extrapolation of T_m^0 values for different optical purities. A ΔH_m value of *ca.* 146 J/g was also reported for the stereocomplex crystals having an infinite thickness [26]. Therefore, the T_m value of the PLLA/PDLA blend (215.9 °C) confirmed that stereocomplex

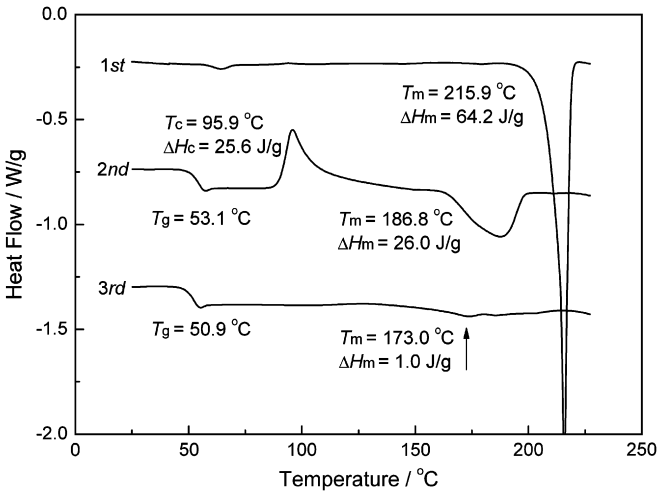

Fig. 1. DSC thermograms of the PLLA/PDLA blend at a heating rate of 10 °C/min. The first run corresponds to the blended sample from solution blending and drying, the second and third ones to samples after quenching in liquid nitrogen from the melt. Before quenching, the sample was kept at 230 °C for 1 min to eliminate all nuclei.

exclusively formed from the blend without homo-crystallization of either PLLA or PDLA, indicating that 50/50 blending benefits stereocomplexation [11].

On the other hand, the T_m values obtained in the second and third runs (186.8 and 173.0 °C) are higher than those of PLLA and PDLA, as shown in Table 1 (165.8 °C and 160.3 °C, respectively). This finding implies that imperfect stereocomplex be formed instead of homo-crystallites. In fact, the corresponding WAXD spectrum (Fig. 2) exhibits three main diffraction peaks at θ values of 5.9, 10.3 and 11.9°, which are characteristic of PLA stereocomplex crystallized in a trigonal unit cell of dimensions: $a = b = 1.498$ nm, $c = 0.870$ nm, $\alpha = \beta = 90°$, and $\gamma = 120°$ [12].

The much lower T_m and ΔH_m values could thus be attributed to highly depressed stereocomplex crystallization in the second and third heating runs. It is commonly assumed PLLA/PDLA blend would exhibit the same melting behaviors. Surprisingly, stereocomplex crystallization significantly decreased in the second run, and almost disappeared in the third run. Fig. 3 depicts the melting behaviors of PLLA subjected to the same thermal treatment for the sake of comparison. Unambiguously, PLLA preserved the same melting behaviors despite the heating/cooling processes, the T_m remaining at *ca.* 165.8 °C. Therefore, thermal degradation could not account for the depression of PLLA/PDLA stereocomplex crystallization in the second and third heating runs. This behavior will be further illustrated by applying various melting conditions at temperatures ranging from 224 to 230 °C, and for different time periods.

Fig. 4A exhibits the cooling heat flows of the PLLA/PDLA blend after 1 min melting at 224 °C, 226 °C and 230 °C, respectively. With melting at 224 °C, the melt crystallization temperature (T_{mc}) appeared at 144.0 °C with ΔH_c of 23.6 J/g. Melting at 226 °C led to a lower T_{mc} at 120.0 °C with a lower ΔH_c of 10.7 J/g. Finally with melting at 230 °C, the melt crystallization was hardly distinguished. T_g remained approximately the same (*ca.* 51 °C) in all cases, while the thermal capacity (ΔC_p) increased from 0.39 J g^{-1} K^{-1} at 224 °C, 0.48 J g^{-1} K^{-1} at 226 °C, to 0.63 J g^{-1} K^{-1} at 230 °C. Higher ΔC_p values imply less crystallinity and higher fraction of amorphous region remaining in the blend.

It is well known that PLLA is a slowly crystallizing material [27]. Miyata and Masuko reported that PLLA remains amorphous when it is cooled from isotropic melt at a rate higher than 10 °C/min [28]. In this work, stereocomplex was formed at a cooling rate of 10 °C/min, thus implying that stereocomplex crystallization is faster than PLLA homo-crystallization. Nevertheless, melt crystallization in the cooling process was distinctly depressed when the blend was melted at higher temperatures. In addition, the subsequent heating process after 224 °C melting exhibits T_m at *ca.* 180 °C for the

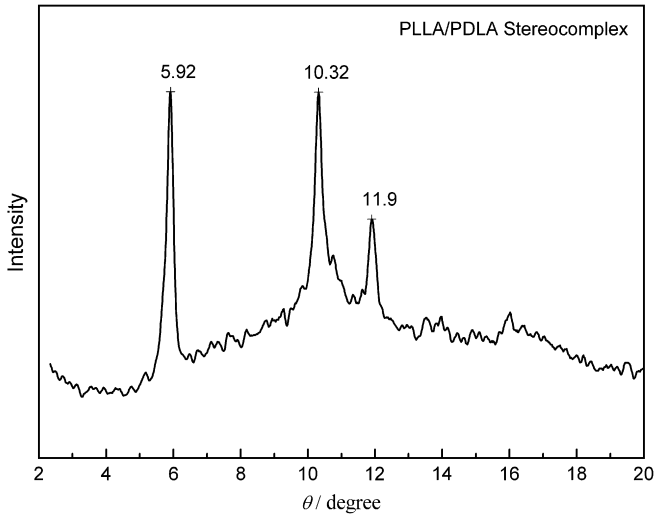

Fig. 2. WAXD spectrum of the PLLA/PDLA blend after crystallization in the second cycle of Fig. 1 (the sample was taken out at 140 °C for WAXD measurements).

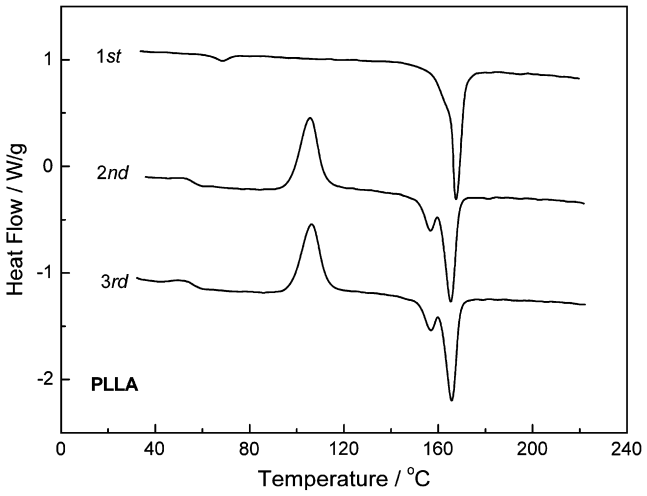

Fig. 3. DSC thermograms of PLLA at a heating rate of 10 °C/min. The first run corresponds to the initial sample, the second and third ones to samples after quenching in liquid nitrogen from the melt. Before quenching, the sample was kept at 230 °C for 1 min to eliminate all nuclei.

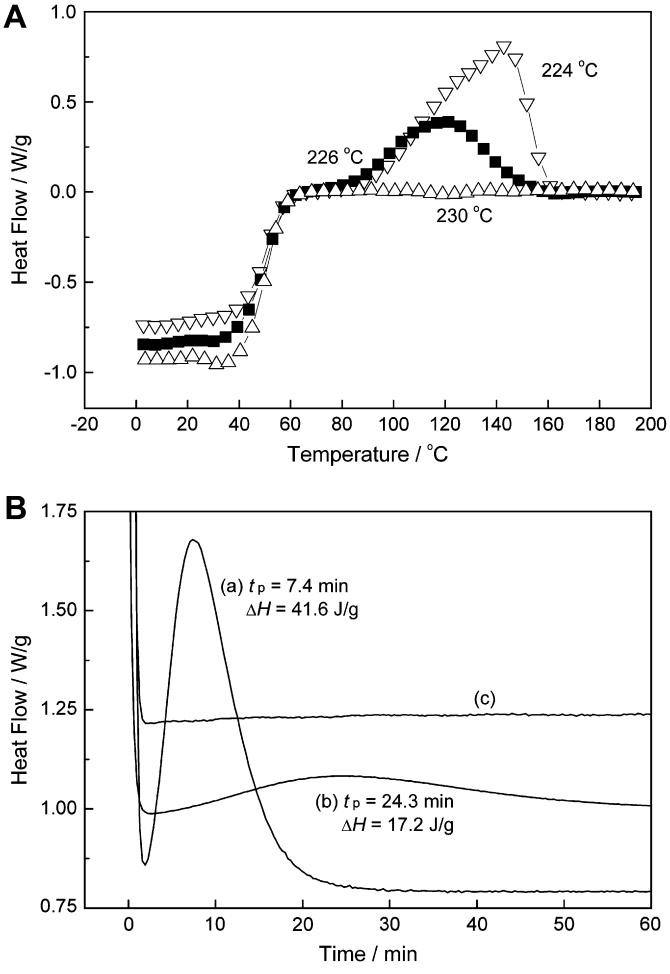

Fig. 4. (A) DSC thermograms of the PLLA/PDLA blend at a cooling rate of 10 °C/min from the melt after 1 min at 230 °C, 226 °C, and 224 °C. (B) Isothermal crystallization at 145 °C after melting at 230 °C for different periods (a, 1 min; b, 2 min; c, 3 min).

crystallized stereocomplex. This result excludes the possibility that 224 °C is not high enough to erase all the crystals and nuclei in the original PLLA/PDLA blend.

The isothermal crystallization behavior of the blend was examined at 145 °C after melting at 230 °C for 1, 2 and 3 min, respectively (Fig. 4B). The crystallization peak is obvious with a peak time (t_p) of 7.4 min and ΔH_c of 41.6 J/g for 1 min melting. After 2 min melting, however, the crystallization ability strongly decreased with a prolonged t_p of 24.3 min and a lower ΔH_c of 17.2 J/g. The isothermal crystallization even disappeared after 3 min melting.

Wang and Mano reported that longer melting period could induce a dramatic crystallinity enhancement of PLLA [29]. However, in this work, longer melting period results in slower crystallization rate and lower degree of crystallization for the PLLA/PDLA blend. Thus, it is of interest to elucidate whether the melting process would influence the microstructure which is one of the key factors determining polymer crystallization.

^{13}C NMR spectroscopy was employed to examine the microstructure of the PLLA/PDLA blend since intermolecular transesterification could influence the crystallization behavior. The blend was first melted at 230 °C for 3 min, quickly cooled to room temperature and then dissolved in $CDCl_3$ for ^{13}C NMR measurements (Fig. 5). Carbonyl carbon resonances were detected at *ca.* 169.6 ppm, and methine and methyl ones at *ca.* 69.0 and 16.6 ppm, respectively. All the carbon fine structures are stereodependent, as previously reported [30,31]. Isotactic LL or DD dyads are noted as i (isotactic), while syndiotactic DL or LD dyads are noted as s (syndiotactic). For example, iiisi denotes chain segments containing 6 lactic units DDDDLL or LLLDD. As shown in Fig. 5, the chain microstructure after 3 min melting at 230 °C is predominantly isotactic. However, other smaller signals were found in terms of hexads in the carbonyl region and tetrads in the methine and methyl regions. In the carbonyl region, the signal at 169.4 ppm is assigned to iiisi, and the one at 169.3 ppm to sisii, isiii and iisii hexads. Similarly, a small isi tetrad was detected in the methine and methyl regions at 69.2 and 16.7 ppm, respectively. The presence of syndiotactic (s) dyads could be ascribed to intermolecular transesterification occurring during the melting process of PLLA/PDLA, although transesterification appeared very limited considering the predominantly isotactic chain microstructure. A transesterification reaction between a PLLA and a PDLA chain leads to a PLLA–PDLA diblock structure, and several transesterification reactions lead to multiblock structures. As reported previously, predominantly multiblock chains resulting from stereoselective ring opening polymerization of DL-lactide are susceptible to stereocomplexation [32,33]. It can be thus concluded that the very limited microstructure change of the PLLA/PDLA blend cannot account for the depression of stereocomplex crystallization.

SEC was used to follow the changes of MW and polydispersity after thermal treatment. No significant changes were detected in either case for the samples used in Fig. 4. Therefore, the different crystallization abilities observed under various melting conditions could not be assigned to MW changes. The findings inspired us to focus on the melt state of the PLLA/PDLA blend.

Fig. 6 presents the morphology of enzymatically etched samples corresponding to those in Fig. 4B. As reported previously, proteinase K preferentially degrades L-lactyl segments as opposed to D-lactyl ones, PDLA being not degradable [34]. And enzymatic degradation in amorphous region precedes that in crystal region of semicrystalline PLA [35]. In Fig. 6A, the crystal morphology corresponding to sample (a) in Fig. 4B is clearly revealed. Lamellae in the spherulites seem to organize in a unique manner which is quite different from PLLA crystallization [36]. Disk-shaped and spherical structures have been observed in the case of stereocomplex formed in acetonitrile solution [37]. Irregular shape of spherulites in Fig. 6A is assigned to spherulite collision which reflects a relatively high degree of crystallinity as evidenced by the ΔH_c value in Fig. 4B-a. The crystal morphology of the etched sample shown in Fig. 6B presents smaller number and size of spherulites, in agreement with strongly depressed isothermal crystallization shown in Fig. 4B. In contrast, Fig. 6C exhibits a kind of network morphology after etching, the amorphous blend being homogeneously etched. The network-like morphology should introduce a hint for the melt state of PLLA/PDLA blend before degradation.

The stereocomplex crystallization behavior seems to strongly depend on the melt state of the PLLA/PDLA blend. As reported recently, crystals can be melted by following the mechanism of

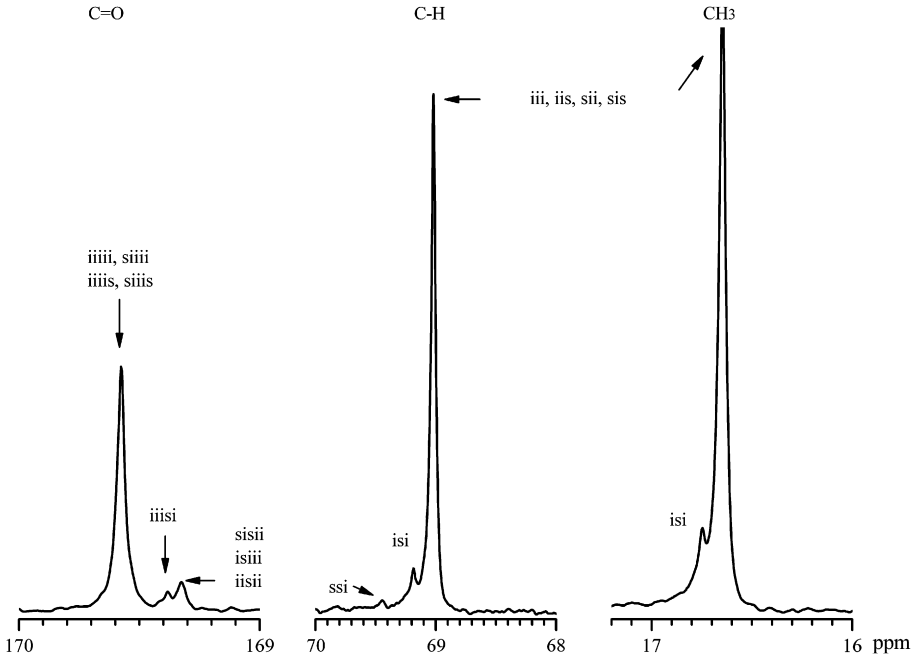

Fig. 5. Carbonyl, methine and methyl regions of the ^{13}C NMR spectrum in $CDCl_3$ of PLLA/PDLA blend after 3 min melting at 230 °C.

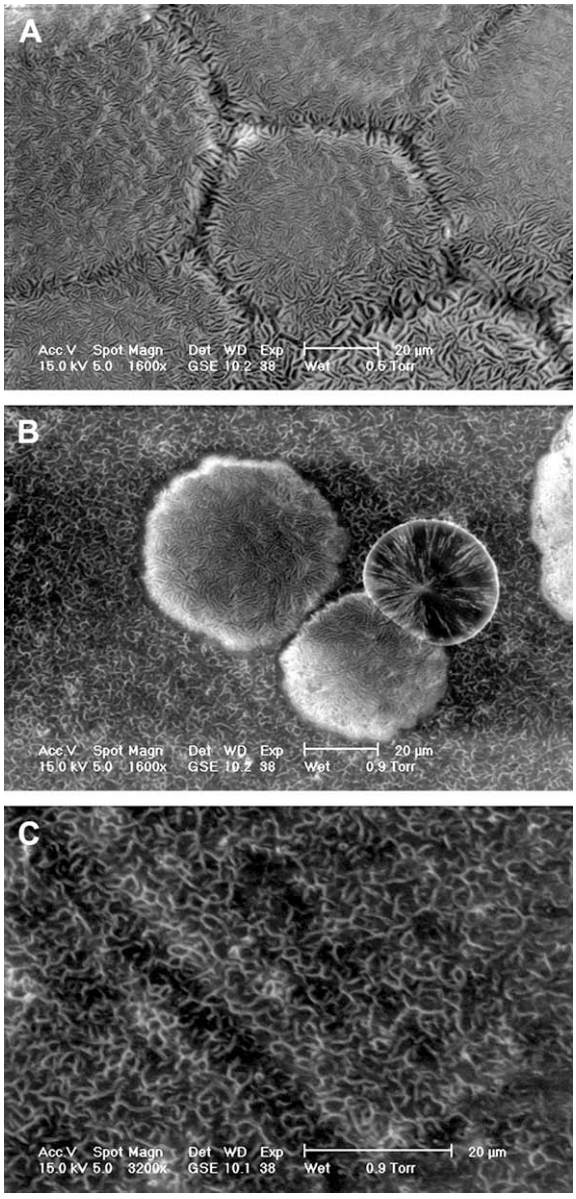

Fig. 6. ESEM micrographs of the enzymatically etched PLLA/PDLA blend which was melted at 230 °C for 1 min (A); 2 min (B) and 3 min (C), followed by isothermal crystallization at 145 °C for 60 min.

either simple consecutive detachment of chain stems from the crystalline substrate or cluster melting (i.e. chain explosion) in which several chain stems are involved [15,16]. Consecutive detachment of chain stems takes place at much lower temperatures than cluster melting. Therefore, melting by consecutive detachment of chain stems and subsequent diffusion would probably result in a different melt state from stereocomplex because of the predominant interactions between PLLA and PDLA chains.

As referred previously, the crystal structure of PLLA/PDLA stereocomplex is trigonal, consisting of subcells with two enantiomorphous, antiparallel chains [12]. PLLA and PDLA stems are arranged alternately taking 3_1 helical conformation in the stereocomplex [12,13]. And van der Waals forces between the hydrogen of CH_3 and the oxygen of O═C of PLA chains with opposite configurations have been suggested to induce chain packing for stereocomplexation [13]. Recently, according to FTIR analysis by Zhang et al., the $CH_3\cdots O{=}C$ hydrogen bonding contributes to the interaction between chains in PLLA/PDLA stereocomplex, and thus constitutes the driving force for the nucleation of stereocomplexation [38]. Consequently, the strong interaction between PLLA and PDLA chains has been confirmed in either case and should also be considered as a factor to influence the melt state from stereocomplex.

Scheme 1 is proposed as a model to illustrate the melt state of PLLA/PDLA stereocomplex in the melting process. When the stereocomplex from solution is slowly melted by consecutive detachment, the parallel and alternate PLLA and PDLA chains are smoothly changed into melt, probably in couples because of the strong interaction between PLLA and PDLA chains as shown in the left part of Scheme 1(A). Meanwhile, PLLA and PDLA chains inter-penetrate randomly in melt from amorphous regions, as shown in the right part of Scheme 1(A). And in the melt state from stereocomplex, chain diffusion and homogenization in spatial distribution would be hindered because of predominant interaction between opposite configurations. A heterogeneous melt is thus formed as schematically presented in Scheme 1(A). Heterogeneous melt being unstable in entropy, it would gradually change to be homogeneous as the melting period extends. One PLLA chain would penetrate through several PDLA chains and form strong interaction regions by $CH_3\cdots O{=}C$ interaction. Additionally, PLLA/PDLA stereocomplex could be melted in chain explosion to yield a homogeneous melt when the melting temperature is much higher. Scheme 1(B) presents such a homogeneous melt.

Accordingly, the crystallization behavior described above could be explained as following. When the temperature is increased and the melting period is prolonged, the melt state from stereocomplex changes from mainly heterogeneous to homogeneous. PLLA and PDLA chains randomly penetrate in melt with homogeneous distribution of strong interaction regions. Crystallization is thus decreased or prevented because PLA chains are eventually confined by predominant interactions between opposite configurations and difficult to diffuse from amorphous part into stereocomplex lattices. Such a homogeneous melt state could be a prerequisite for the network-like morphology detected in Fig. 6C. Schmidt and Hillmyer used polylactide stereocomplex crystallites as nucleating agents for PLLA crystallization, and attributed the decreased extent of crystallization to the hindered mobility of PLLA chains due to tethering by the stereocomplex [39]. According to the above model, it could be the strong interactions randomly distributed between PLLA and PDLA chains which hinder the crystallization, instead of the stereocomplex itself.

The hypothesis of homogenization of the heterogeneous melt in PLLA/PDLA blend was further confirmed by a complementary experiment. After melting at 230 °C for 3 min, the blend became homogeneous and lost the capability of crystallization. Then the sample was dissolved in dichloromethane. After evaporation of the solvent, a stereocomplex was formed again, as evidenced by DSC (data not shown). This finding indicates that the homogeneous melt recovered its crystallizability via dissolution.

Therefore, the model proposed above appears reasonable to elucidate the unique crystallization behavior of PLLA/PDLA stereocomplex. Further investigations are underway to better

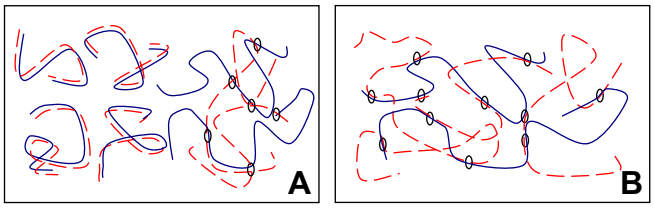

Scheme 1. (A) Heterogeneous melt resulted from consecutive detachment of PLLA/PDLA stereocomplex chain stems together with amorphous region; (B) homogeneous melt resulted from cluster melting and/or from homogenization of heterogeneous melt. The circles represent strong interaction locations of PLLA/PDLA chains.

understand this behavior by using other techniques including small angle neutron scattering (SANS) and rheological measurements.

4. Conclusion

Stereocomplex is exclusively formed from blends of PLLA and PDLA (50/50) with relatively low molecular weights. The crystallization behavior of the PLLA/PDLA blend depends on its initial melt state. When higher temperature and longer period are applied, stereocomplexation is strongly depressed. A model is proposed on the basis of the theory of heterogeneous and homogeneous melts, together with the predominant interactions between PLLA and PDLA chains. This model could explain the unique crystallization behavior depending on the initial melt state. It is assumed that PLLA and PDLA chain couples would preserve their interactions (melt memory) when the stereocomplex crystal melts smoothly, thus resulting in a heterogeneous melt which can easily crystallize. The melt could gradually become homogeneous at higher temperature or longer melting time. The strong interactions between PLLA and PDLA chain segments are randomly distributed in a homogeneous melt, thus preventing subsequent stereocomplex crystallization. However, the homogeneous melt can recover its ability to crystallize via dissolution in a solvent. The relationship between polymer melt state and its crystallizability reported herein could help to predict the behavior of other polymeric stereocomplexes.

Acknowledgements

The authors are indebted to the Project ARCUS 2006 Languedoc-Roussillon/China and to the Shanghai Leading Academic Discipline Project (No. B113) for financial support.

References

[1] Drumright RE, Gruber PR, Henton DE. Adv Mater 2000;12:1841–6.
[2] Li SM, Vert ME. In: Mathiowitz E, editor. The encyclopedia of controlled drug delivery. New York: John Wiley & Sons; 1999. p. 71–92.
[3] Ikada Y, Jamshidi K, Tsuji H, Hyon SH. Macromolecules 1987;20:904–6.
[4] Fukushima K, Chang YH, Kimura Y. Macromol Biosci 2007;7:829–35.
[5] Tsuji H. Biomaterials 2003;24:537–47.
[6] Li SM, Vert M. Macromolecules 2003;36:8008–14.
[7] Sodergard NDA, Stolt EM, Siistonen HK, Nobes GAR. US Patent UP20080207840; 2008.
[8] Hiruma T, Yamada T, Muta T. WIPO Patent WO2008096798; 2008.
[9] Tsuji H. Macromol Biosci 2005;5:569–97.
[10] Tsuji H, Tezuka Y. Biomacromolecules 2000;5:1181–6.
[11] Tsuji H, Ikada Y. Macromolecules 1993;26:6918–26.
[12] Cartier L, Okihara T, Lotz B. Macromolecules 1997:6313–22.
[13] Brizzolara D, Cantow HJ, Diederichs K, Keller E, Domb AJ. Macromolecules 1996;29:191–7.
[14] Rastogi S, Lippits DR, Peters GWM, Graf R, Yao YF, Spiess HW. Nat Mater 2005;4:635–41.
[15] Lippits DR, Rastogi S, Hohne GWH, Mezari B, Magusin PCM. Macromolecules 2007;40:1004–10.
[16] Lippits DR, Rastogi S, Hohne GWH. Phys Rev Lett 2006;96:218303.
[17] Strobl G. The physics of polymers: concepts for understanding their structures and behavior. 2nd ed. Berlin: Springer-Verlag; 1997.
[18] Okada T, Saito H, Inoue T. Macromolecules 1992;25:1908–11.
[19] Lotz B. Adv Polym Sci 2005;180:17–44.
[20] Muthukumar M. Adv Polym Sci 2005;191:241–74.
[21] Lorenzo AT, Arnal ML, Sanchez JJ, Muller AJ. J Polym Sci B Polym Phys 2006; 44:1738–50.
[22] Massa MV, Lee MSM, Dalnoki-Veress K. J Polym Sci B Polym Phys 2005; 43:3438–43.
[23] Schneider S, Drujon X, Lotz B, Wittmann JC. Polymer 2001;42:8787–98.
[24] He Y, Fan ZY, Wei J, Li SM. Polym Eng Sci 2006;46:1583–9.
[25] He Y, Fan ZY, Hu YF, Wu T, Wei J, Li SM. Eur Polym J 2007;43:4431–9.
[26] Tsuji H, Horii F, Nakagawa M, Ikada Y, Odani H, Kitamaru R. Macromolecules 1992;25:4114–8.
[27] Garlotta D. J Polym Environ 2001;9:63–84.
[28] Miyata T, Masuko T. Polymer 1998;22:5515–21.
[29] Wang YM, Mano JF. Eur Polym J 2005;41:2335–42.
[30] Bero M, Dobrzynski P, Kasperczyk J. J Polym Sci A Polym Chem 1999;37: 4038–42.
[31] Schwach G, Coudane J, Engel R, Vert M. Polym Bull 1994;32:617–23.
[32] Hu JL, Tang ZH, Qiu XY, Pang X, Yang YK, Chen XS, et al. Biomacromolecules 2005;6:2843–50.
[33] Pang X, Du HZ, Chen XS, Zhuang XL, Cui DM, Jing XB. J Polym Sci A Polym Chem 2005;43:6605–12.
[34] Reeve MS, McCarthy SP, Downey MJ, Gross RA. Macromolecules 1994;27: 825–31.
[35] Li SM, McCarthy S. Macromolecules 1999;32:4454–6.
[36] He Y, Wu T, Wei J, Fan ZY, Li SM. J Polym Sci B Polym Phys 2008;46: 959–70.
[37] Tsuji H, Hyon SH, Ikada Y. Macromolecules 1992;25:2940–6.
[38] Zhang J, Sato H, Tsuji H, Noda I, Ozaki Y. Macromolecules 2005;38: 1822–8.
[39] Schmidt SC, Hillmyer MA. J Polym Sci B Polym Phys 2001;39:300–13.